Ambivalent Role of Rotamers in Cyclic(alkyl)(amino)carbene Ruthenium Complexes for Enantioselective Ring-Opening Cross- Metathesis

Jennifer Morvan, François Vermersch, Ziyun Zhang, Thomas Vives, Thierry Roisnel, Christophe Crévisy, Laura Falivene, Luigi Cavallo, Nicolas Vanthuyne, Guy Bertrand, et al.

Ambivalent Role of Rotamers in Cyclic(alkyl)(amino)carbene Ruthenium Complexes for Enantioselective Ring-Opening Cross-Metathesis

Jennifer Morvan, François Vermersch, Ziyun Zhang, Thomas Vives, Thierry Roisnel, Christophe Crévisy, Laura Falivene, Luigi Cavallo, Nicolas Vanthuyne, Guy Bertrand,* Rodolphe Jazzar,* and Marc Mauduit*

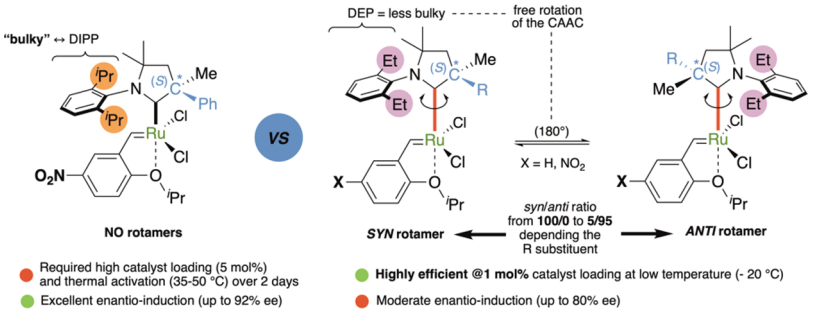

ABSTRACT: The development of highly efficient enantioselective olefin metathesis catalysts is a significant challenge. Using optically pure chiral cyclic (alkyl)(amino)carbene (ChiCAAC) ligands combined with preliminary mechanistic insights and density functional theory (DFT) computations, we show that catalytic performances in this field can be impaired by the formation of rotamers before the enantio-determining step. Using DFT, we also demonstrate that these results can help accelerate the process of ligand discovery by providing faster methods to discriminate potential candidates.

INTRODUCTION

"Catalysts are the conductors who choreograph the chemical dance that results in the formation of new structures"

R. H. Grubbs—Nobel Lecture—2005.[1]

In 2007, Bertrand, Grubbs, and co-workers demonstrated that this symphony could greatly benefit from the use of cyclic(alkyl)(amino)carbenes (CAACs)[2] as ligands for ruthenium-catalyzed olefin metathesis (Figure 1).[3] Since then, CAAC ligands have been shown to afford robust ruthenium precatalysts with remarkable catalytic performances in a number of metathesis transformations.[4,5] Their growing popularity has been attributed to the highly modular steric environment of the CAAC framework[6] and their propensity to generate stable, yet very reactive, catalysts. Using a new class of CAACs, namely, chiral cyclic(alkyl)(amino)carbenes (ChiCAACs),[7] we recently extended their application to asymmetric olefin metathesis.[8,9] To overcome the synthetic drawback plaguing chiral ligands and catalyst preparation (complex/low-yielding procedures), meanwhile facilitating the screening of CAAC-Ru catalysts, we capitalized on preparative high-performance liquid chromatographic resolution (^{Prep}HPLC), a technology very popular in the industrial setting.[10] Despite this strategy and another recent one,[11] streamlining a chiral ligand design to achieve high enantioselectivity across a broad range of substrates remains challenging. Arguably, a great deal of ligand optimization for specific applications lies in our understanding of the various structural features that affect stereo- and/or enantioselectivity.[12] Herein, capitalizing on an experimental and computational approach, we report a comprehensive investigation of the catalytic activity of optically pure diethylphenyl (DEP) *N*-substituted CAAC ruthenium complexes in asymmetric ring-opening cross-metathesis (AROCM) reactions (Figure 2).[13] This work allowed us to identify the enantio-determining step for this process, which proved critical to discriminate putative ligand frameworks that would not yield significant improvement. It should be noted that these studies remain rare even in well-studied NHC-catalyzed asymmetric olefin metathesis.[13d,14]

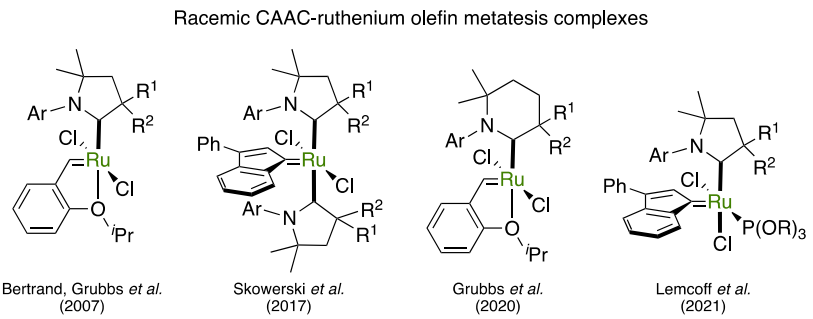

Figure 1. State-of-the-art CAAC-Ru olefin metathesis catalysts.

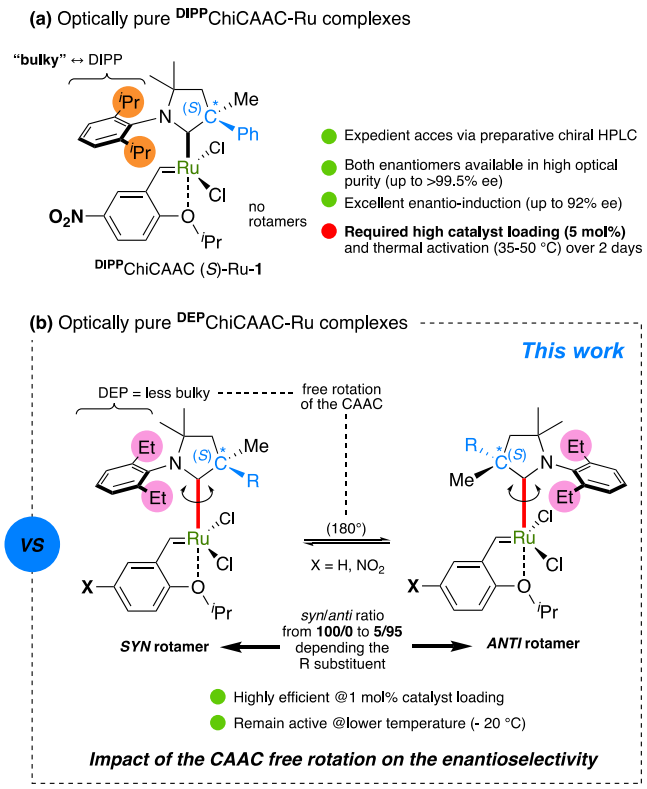

Figure 2. (a) DIPP ChiCAAC-Ru complexes as ligands for asymmetric olefin metathesis catalysts. (b) Ambivalent catalytic activities of optically pure DEP ChiCAAC-Ru complexes (this work).

RESULTS AND DISCUSSION

We began our investigation with readily accessible air-stable DEP ChiCAAC-**Ru-2**−**8** complexes, featuring structural variations through the stereogenic quaternary carbon center substituents (phenyl, 1-naphthyl, 2-naphthyl, 3,5-dimethylphenyl, and cyclohexyl), while considering nitro-substituted Hoveyda−Grubbs metathesis catalysts.[15] As depicted in Scheme 1, chiral CAAC precursors were synthesized in good overall yields over four steps, ranging from 41 to 74%. The corresponding complexes were obtained in low-to-good isolated yields after purification over silica gel (7−76% yield).[16] We next studied their resolution by preparative chiral HPLC and found Chiralpak IE or IF to afford the best resolution using a mobile phase consisting of a heptane/ethanol/dichloromethane mixture (70/10/20 ratio).[17] Under these conditions, excellent elution time and good loading capacity allowed for the antipode separation of (*rac*)-**Ru-2** on a

Scheme 1. Synthesis of DEP ChiCAAC Precursors and Related Ruthenium Complexes[a,b,c]

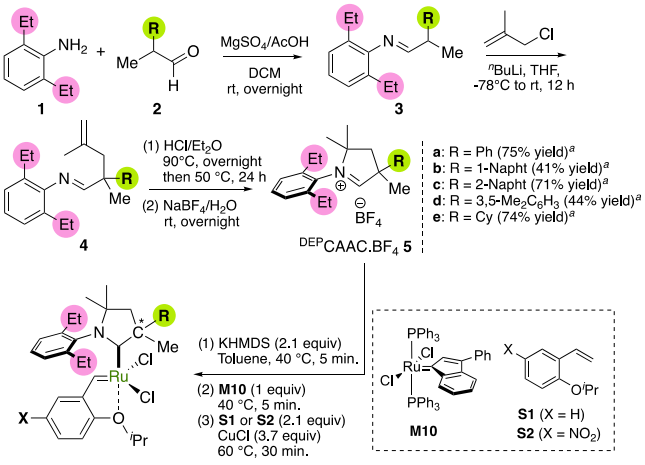

Ru-2: R = Ph, X = H (83% yield)[b]
syn/*anti* ratio: **70/30**[c]
Ru-3: R = 1-Naphthyl, X = H (53% yield)[b]
syn/*anti* ratio: **5/95**[c]
Ru-4: R = Ph, X = NO_2 (74% yield)[b]
syn/*anti* ratio: **75/25**[c]
Ru-5: R = 1-Naphthyl, X = NO_2 (7% yield)[b]
syn/*anti* ratio: **5/95**[c]
Ru-6: R = 2-Naphthyl, X = NO_2 (56% yield)[b]
syn/*anti* ratio: **70/30**[c]
Ru-7: R = 3,5-$Me_2C_6H_3$, X = NO_2 (72% yield)[b]
syn/*anti* ratio: **70/30**[c]
Ru-8: R = Cy, X = NO_2 (71% yield)[b]
syn/*anti* ratio: **100/0**[c]

[a]Overall isolated yields over four steps. [b]Isolated yields from ChiCAAC precursors **5**. [c]Ratio determined by ^{1}H NMR spectroscopy in $CDCl_3$.

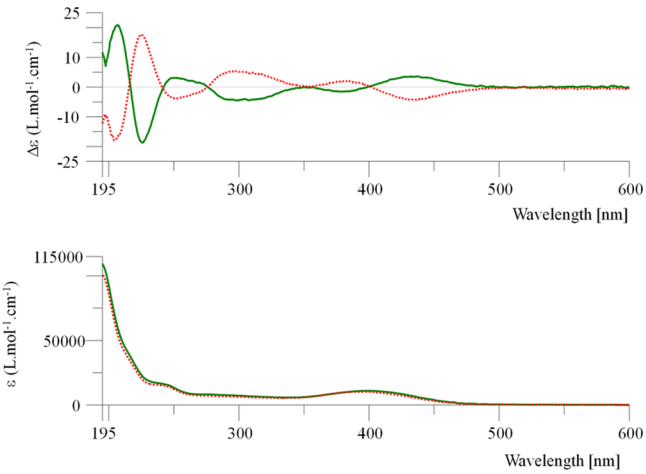

Figure 3. Electronic circular dichroism (ECD) (a) and UV spectra (b) of the first eluted (+)-**Ru-2** (solid line) and second eluted (−)-**Ru-2** (dotted line).

Scheme 2. (a) Chiral Preparative HPLC Resolution of ^{DEP}ChiCAAC Ruthenium Complexes (*rac*)-Ru-2-8 and (b) Solid-State Structures of ^{DEP}ChiCAAC-Ru Complexes Ru-2,-8[a,b,c]

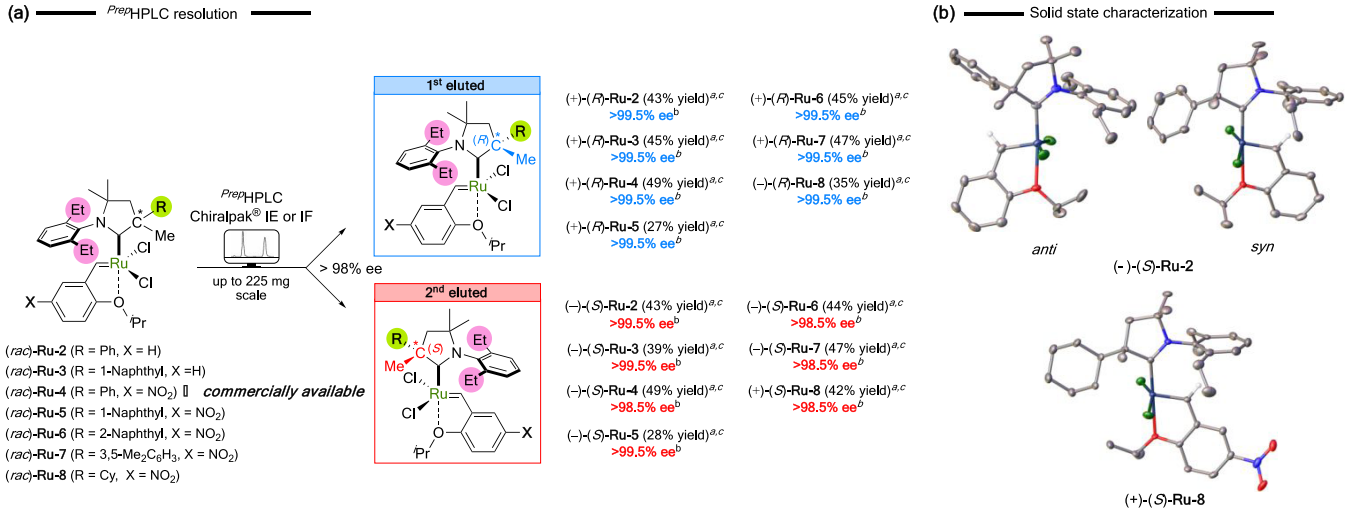

[a]Isolated yield after preparative chiral resolution. [b]Determined by chiral stationary-phase HPLC analysis. [c]*Syn*/*anti* ratios remained unchanged after the chiral resolution. Displacement ellipsoids are drawn at 50% probability

Table 1. Evaluation of Optically Pure Ru-1−9 Complexes in Catalytic AROCM of Norbornene S1a[a]

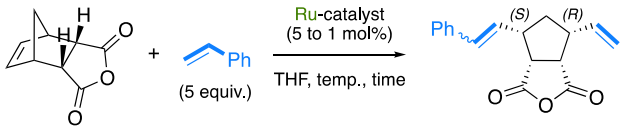

S1a P1a

entry	Ru-**cat** (mol %)	*T* (°C)/time	conv.[b] (yield)[c] (%)	*E*/*Z* ratio[d]	Ee (*E*)-**P1a** (%)[e]
1	(*S*)-**1** (5)	35/2d	99 (41)	85/15	90 (*S*,*R*)
2	(*S*)-**2** (1)	rt/1 h	99 (64)	85/15	60(*S*,*R*)[f]
3	(*R*)-**2** (1)	rt/1 h	99 (64)	85/15	60 (*R*,*S*)
4	(*R*)-**3** (1)	rt/6 h	99 (47)	75/25	60 (*R*,*S*)
5	(*R*)-**4** (1)	rt/0.25 h	99 (57)	85/15	61 (*R*,*S*)
6	(*R*)-**4** (1)	0/0.75 h	99 (61)	85/15	65 (*R*,*S*)
7	(*R*)-**4** (1)	−10/1.7 h	99 (56)	85/15	68 (*R*,*S*)
8	(*R*)-**4** (1)	−20/4 h	99 (54)	85/15	70 (*R*,*S*)
9[g]	(*R*)-**4** (2)	−30/1d	99 (52)	80/20	71(*R*,*S*)[h]
10	(*R*)-**5** (1)	rt/1.5 h	99 (37)	75/25	60 (*S*,*R*)
11	(*R*)-**6** (1)	rt/0.5 h	99 (66)	90/10	74 (*R*,*S*)
12	(*R*)-**7** (1)	rt/0.25 h	99 (70)	90/10	58 (*R*,*S*)
13	(*R*)-**8** (1)	rt/1 h	99 (75)	99/1	49 (*R*,*S*)
14	(*R*)-**6** (1)	−20/20 h	99 (63)	90/10	80 (*R*,*S*)
15	(*R*)-**9** (5)	55/4d	20 (nd)	80/20	66 (*R*,*S*)

[a]Reaction conditions: [Ru] catalyst (5−1 mol %), styrene (5 equiv), and THF (0.15 M). [b]Conversions were monitored by ^{1}H NMR spectroscopic analysis. [c]Isolated yields after column chromatography (note that **P1a** is prone to decomposition during purification). [d]*E*/*Z* ratio determined by SFC on the crude mixture. [e]ee determined by SFC on a chiral stationary phase. [f]Absolute configuration determined on the corresponding diol (see SI for details). [g]Reaction performed in 2-MeTHF. [h]ee of (*Z*)-**P1a**: 18%. nd: not determined.

preparative scale (225 mg; flow rate = 5 mL.min^{-1}) (Figure 3; see the Supporting Information (SI) for details). Both (+)-**Ru-2** (first eluted) and (−)-**Ru-2** (second eluted) enantiomers were isolated in excellent 43−45% yields and remarkable enantiomerical purities (>99.5%). To our delight, using the aforementioned conditions, complexes **Ru-3**−**8** were successfully resolved (up to 225 mg scale), and their respective (+)- and (−)-enantiomers were obtained in good yields (from 24 to 49%) and excellent optical purities (up to >99.5% ee) (Scheme 2)).

Note that the methodology is amenable to the commercially available ^{DEP}ChiCAAC-**Ru-4** complex, which was equally resolved in a nearly quantitative yield and excellent ees.[18] We unambiguously confirmed the absolute configuration of the second eluted **Ru-2,-4,-7,-8** complexes by an X-ray diffraction study (*S*, Scheme 2),b and SI). We tentatively attributed the same (*S*) configuration to the second eluted **Ru-3,-5** for which crystals suitable for an X-ray diffraction study could not be obtained. Note that in the case of the complex (*S*)-**Ru-2**, the rotational isomer (*anti*) featuring the quaternary chiral center

Scheme 3. Synthesis of the Optically Pure Bis-iodo ^{DEP}ChiCAAC Ruthenium Complex (*R*)-Ru-9

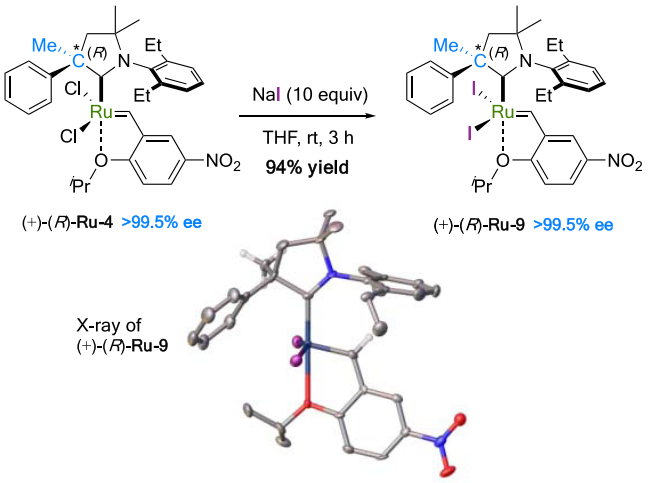

above the styrenyl-ether moiety was also observed in the solid state.[19]

Having obtained a small library of optically pure ChiCAAC–ruthenium complexes with full structural information, we proceeded to investigate their catalytic performances in asymmetric olefin metathesis transformations.[9]

Reaction Optimization. As a benchmark reaction, we considered the asymmetric ring-opening cross-metathesis (AROCM) reaction of himic anhydride, the *meso*-norbornene derivative S1a.[13] The reaction was performed in THF and in the presence of 5 equiv of styrene (Table 1). Compared with ^{DIPP}Ru-(*S*)-**1** (entry 1), ^{DEP}Ru complexes (*S*) and (*R*)-**2** demonstrated enhanced reactivity at 1 mol % and decreased enantioselectivity (entries 2 and 3). Switching the phenyl with 1-naphtyl at the quarternary carbon led to a significant loss of reactivity and *E*/*Z* selectivity (entry 4). We next considered a Grela-type variant (*R*)-**4** bearing an activating *p*-nitro styrenylether, which gratifyingly led to a significant improvement of the reactivity (entry 5). In this case, a lower temperature or longer reaction time did not significantly improve the *E*/*Z* ratio or the enantioselectivity (entries 6–9).

Probing various substitutions at the α-quarternary carbon allowed us to identify 2-naphtyl (*R*)-**6** as an ideal middle point between reactivity and selectivity despite cyclohexyl (*R*)-**8** yielding excellent *E*/*Z* selectivity (99:1) (entries 10–13). Using this catalyst and performing the reactivation at a lower temperature, albeit with a longer reaction time, resulted in a good *E*/*Z* ratio and enantioselectivity (entry 14). Note that we also evaluated the optically pure bis-iodo ruthenium complex (*R*)-^{DEP}**Ru-9**, which is conveniently accessible from (*R*)-^{DEP}**Ru-4** (Scheme 3). Unexpectedly this substitution led to a significant loss of catalytic activity without any improvement of enantioselectivity (entry 15).[20]

Reaction Scope. Having identified **Ru-6** as the most efficient catalyst in the AROCM of norbornene, we evaluated its scope across a range of norbornenes **S1–2** and cyclopropene **S3**[13] (Scheme 4). To our delight, reacting *endo*-norbornene with either electron-rich or electron-poor styrenes led to the formation of AROCM products **P1b** and **P1c** with good *E*-selectivity and enantioselectivity, whereas protected diol substrates led to a significant loss of enantioselectivity (**P1d–f**). In contrast to these results, the *exo*-norbornene **S2** resulted in a decrease in the isolated yield and selectivity, with a noticeable switch in the *E*/*Z* selectivity in favor of the *Z* isomer in most cases (**P2a–i**).[21] With diol **S2c**, we confirmed using **Ru-8** that the configuration of the ligand is a determining factor to control both the *E*/*Z* selectivity and the enantioselectivity. Finally, we diverted our attention to the AROCM of cyclopropene **S3** using a range of terminal olefins and ^{DEP}ChiCAAC catalysts. Styrene furnished the desired product **P3a** in excellent yields with all catalysts tested. Interestingly, good enantioselectivity was obtained for the *Z* isomer despite the lower *E*/*Z* selectivity of the reaction. In contrast to these results, switching to allyl acetate resulted in a decrease in both the reactivity and the selectivity for **P3b** irrespective of the catalysts tested.

Given the significant loss of enantioselectivity observed between ^{DIPP}**Ru-1** and ^{DEP}**Ru-2** (Table 1, entries 1 and 2), we next wondered whether the *syn*- and *anti*-rotational isomers observed during the solid-state characterization of the complex (*S*)-**Ru-2** could help rationalize this difference.

Mechanistic Considerations. Using NMR spectroscopy, we first evaluated whether the **Ru-2** *syn*- and *anti*-rotational isomers could also be observed in solution. As shown in Figure 4, a 70:30 ratio was observed by ^{1}H NMR spectroscopy at room temperature.[19] The nuclear Overhauser effect (nOe) between the prominent alkylidene proton $\mathbf{H_a}$ and the aryl ethyl groups (Tol-D_8 at −20 °C) unambiguously established *syn*-**Ru-2** as the major isomer. Meanwhile, nOe between the alkylidene proton $\mathbf{H_b}$ and the methyl group of the stereogenic center confirmed the spatial conformation of the *anti*-**Ru-2** minor isomer. To better understand this dynamic conformational behavior, a variable-temperature ^{1}H-NMR spectroscopy study ranging from −40 to 100 °C was performed. As shown in Figure 4, slow coalescence of benzylidene protons of both *syn* ($\mathbf{H_a}$, 16.4 ppm) and *anti* ($\mathbf{H_b}$, 17.9 ppm) isomers was observed around 60 °C, leading to a broad singlet at 17 ppm. Similarly, at lower temperatures (−10 to −40 °C), a higher refinement of benzylidene protons was observed in line with a slower rotation of the ruthenium–carbene bond.

As summarized in Table 2, the same dynamic behavior was observed in other DEP-substituted complexes **Ru-4,6-8** but not with DIPP-substituted complexes **Ru-1a,b** (Figure 1, and entries 1 and 2) even at low temperatures. Altogether, these observations support a higher rotational barrier of 2,6-diisopropylaniline compared with 2,6-diethylaniline substituents, which likely originates from an increased steric environment.

The same rationale also applies to ^{DEP}ChiCAAC-**Ru-3,5** bearing a 1-naphtyl substituent, which showed a *syn*/*anti* mixture in solution (entries 5 and 6), whereas only the *syn* isomer was observed for the more sterically hindered ^{DEP}**Ru-8** bearing the cyclohexyl substituent (entry 9). DFT showed the *anti*-isomer of ^{DIPP}**Ru-1a,b** to be 3–5 kcal/mol higher in energy than the *syn*-isomer. In contrast, a smaller $\Delta\Delta G_{syn/anti}$ (less than 2 kcal/mol) was calculated for ^{DEP}**Ru-2-7** in line with the equilibrium observed by NMR spectroscopy. For ^{DEP}**Ru-8**, the *syn*-isomer is about 4.8 kcal/mol more stable, which is in agreement with a more steric environment. Finally, with ^{DEP}**Ru-3** and **5**, the *anti*-isomer is more accessible by up to 1.4–1.5 kcal/mol, which can be rationalized by the steric clash between the terminal -CH_3 of the ethyl groups on the DEP and the 1-napthyl moiety (3.4–3.5 Å for the *syn*-isomer and 3.9 Å for the *anti*-isomer). Altogether, DFT calculations and

Scheme 4. Scope of AROCM Catalyzed by Optically Pure ^{DEP}ChiCAAC-Ru Complexes[a,b,c,d,e,f,g,h,i,j]

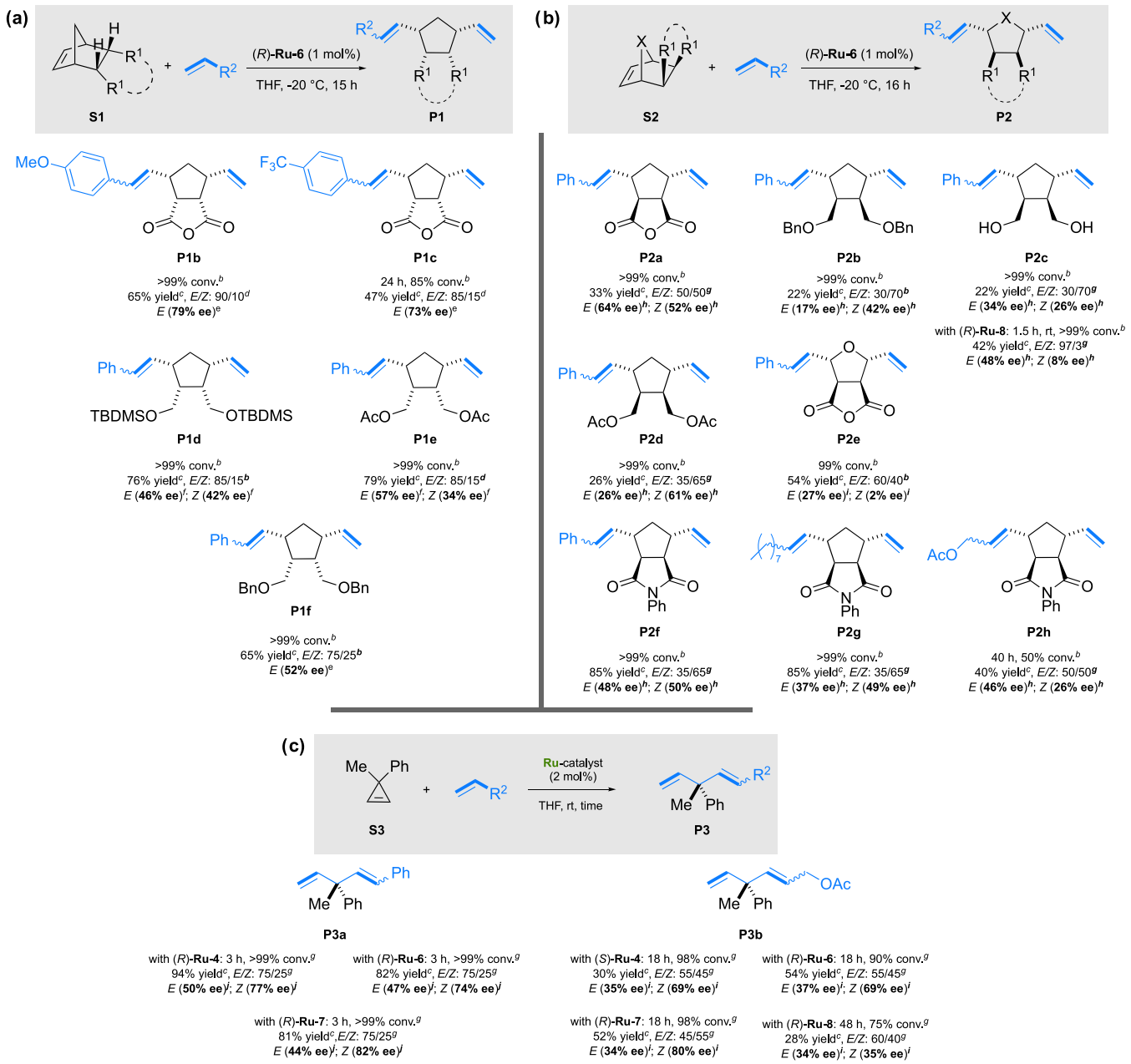

[a]Reaction conditions: [Ru] catalyst (2 to 1 mol %), terminal olefin (5 equiv), THF (0.1M). [b]Determined by 1H NMR spectroscopic analysis. [c]Isolated yields after column chromatography (Note that **P2a−e** and **P3b** are prone to rapid decomposition during purification). [d]Determined by SFC on the crude mixture. [e]Determined by SFC on a chiral stationary phase (see SI for details). [f]Determined on the corresponding diol by SFC on a chiral stationary phase. [g]Determined by GC-MS. [h]Determined by HPLC on a chiral stationary phase. [i]Determined on the corresponding alcohol by HPLC on a chiral stationary phase. [j]Determined by GC on a chiral stationary phase.

experimental results suggest that the *syn* and *anti* configurations in these complexes are strictly under steric control.

DFT Studies. To rationalize these results, a mechanistic study of AROCM with norbornenes catalyzed by (*S*)-^{DEP}**Ru-4** was performed using DFT (Scheme 5A). Having observed the formation of *p*-nitro styrenylether in the reaction media resulting from the activation of the precatalyst with styrene (see SI for details), we considered the propagation to involve a benzylidene intermediate.[13a] Because of the chiral environment of ChiCAACs with C_1-symmetry,[19] we also considered two different geometries to account for the formation of a metallacyclobutane with inversion at the Ru center. $\mathbf{A}_{syn}$ results from the *anti*-rotamer (*S*)-^{DEP}**Ru-4** that features the benzylidene in the apical position to the quaternary chiral center, and $\mathbf{A}_{anti}$ results from the *syn*-rotamer (*S*)-^{DEP}**Ru-4** in which the benzylidene unit is in the apical position to the *N*-DEP moiety. With these structural features in mind, two catalytic cycles are proposed, which account for the enantio- and diastereo-determining steps. Starting from the catalytically active propagating Ru-benzylidene species **A**, coordination of the norbornene substrate **S1** occurs trans to the ChiCAAC ligand, leading to transient intermediates **Bn** (*syn*, *n* = 1, 2 and *anti*, *n* = 3, 4) that are approximately 7 and 11 kcal/mol higher in energy with respect to $\mathbf{A}_{syn}$ (set as the zero-point energy

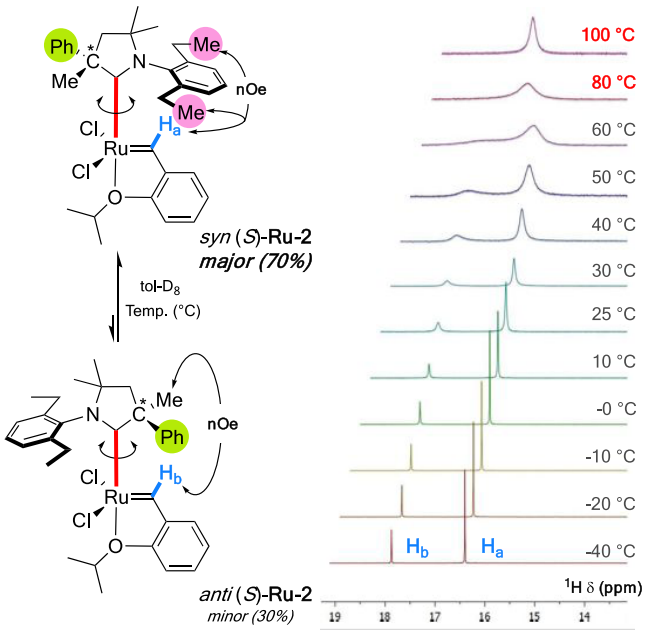

Figure 4. ^{1}H-NMR of *syn* (major) and *anti* (minor) rotational isomers of (+)-(*S*)-Ru-**2** evidencing the free/frozen rotation of ChiCAAC ligand depending on the temperature.

Table 2. Conformer analysis of ^{DIPP}ChiCAAC- vs ^{DEP}ChiCAAC-containing Ru precatalysts supported by DFT

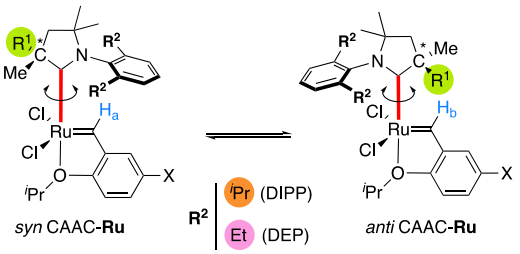

entry	Ru-complex	R^1	X	*syn*/*anti* ratio[a]	$\Delta\Delta G$[b]
1	^{DIPP}Ru-**1a**	Ph	H	100/0	3.5
2	^{DIPP}Ru-**1b**	Ph	NO_2	100/0[c]	4.5
3	^{DEP}Ru-**2**	Ph	H	70/30	0.3
4	^{DEP}Ru-**4**	Ph	NO_2	75/25	0.8
5	^{DEP}Ru-**3**	1-naphthyl	H	5/95	−1.4
6	^{DEP}Ru-**5**	1-naphthyl	NO_2	5/95	−1.5
7	^{DEP}Ru-**6**	2-naphthyl	NO_2	70/30	1.1
8	^{DEP}Ru-**7**	3,5-$Me_2C_6H_3$	NO_2	70/30	0.8
9	^{DEP}Ru-**8**	Cy	NO_2	100/0	4.8

[a]Determined by ^{1}H NMR spectroscopy. [b]$\Delta\Delta G$ (*anti*-*syn*) in THF (kcal/mol). See SI for details.

reference) for the *syn*- and *anti*-pathways, respectively (Scheme 5B). We focused on the metallacycle forming and opening transition states affecting the *E*/*Z* selectivity and enantioselectivity of the reaction.[8a] The ensuing ring-opening of the resulting metallacycle **Cn** proceeds via transition states **Cn**-**Dn**, leading to the opening of the six-membered ring of the norbornene substrate. The energy profiles for the *E*-selective pathways are illustrated in Scheme 5 for both propagating Ru-benzylidene species $\mathbf{A}_{anti}$ and $\mathbf{A}_{syn}$ (see SI for reaction *Z*-selective pathways). In the case of $\mathbf{A}_{syn}$, the ring-closing step **B** → **C** requires overcoming energy barriers of 10.8 and 11.6 kcal/mol, calculated from the $\mathbf{A}_{syn}$ species, for the formation of the *S*,*R* and *R*,*S* products, respectively. The resulting intermediate **C** would preferentially continue forward to **D** as the ring-opening step **C** → **D** occurs easily (~5 kcal/mol from the corresponding intermediate **C**). This indicates that the enantio-determining step involves the metallacycle-forming transition state **Bn-Cn** ($\mathbf{TS}_{syn}$) along *E*-selective pathways. The same is also observed from $\mathbf{A}_{anti}$, where the enantio-determining transition states $\mathbf{TS}_{anti}$ require overcoming energy barriers of 14.7 (**B3-C3**) and 13.4 (**B4-C4**) kcal/mol for the formation of the *S*,*R* and *R*,*S* enantiomers, respectively. These results can be rationalized by considering favorable interactions during the respective transition states. As shown in Scheme 5C, the favored transition states **Bn-Cn** (**n** = **1** and **4**) mitigate steric clash between the norbornene heterocycle and the carbene ligand located in the apical position. Altogether, our DFT model ascertains that the catalytic cycle proceeds mainly via $\mathbf{A}_{syn}$. This is in good agreement with the moderate ee observed for (*E*)-(*S*,*R*) compounds (as a result of the small energy difference between **B1-C1** and **B2-C2**; 0.8 kcal/mol). Note that the accessible $\mathbf{A}_{anti}$ and (*E*)-(*R*,*S*)-selective alternative pathway could likely justify a decrease in ee on increasing the reaction temperature. More interestingly, these results can help rationalize the increased enantio-induction observed with the more sterically hindered 2-naphthyl precursor ^{DEP}**Ru-6** (80% ee; Table 1; entry 14). In this case, we found a slightly higher $\Delta\Delta G^{\ddagger}$ = 1.5 kcal/mol (Figure 5) for the two competing **B1-C1** and **B2-C2** transition states (vs 0.8 kcal/mol and 70% ee for ^{DEP}**Ru-4**; entry 8).

To improve the selectivity further, we used DFT modeling to predict the outcome of ligand modification at the chiral quaternary carbon of the ChiCAAC ligand. As shown in Figure 5, increasing the steric environment further through 3,5-$^{t}Bu_2C_6H_3$ is not predicted to yield any significant improvement in the enantioselectivity with respect to the (*S*)-^{DEP}**Ru-4** catalyst. In fact, the *tert*-butyl groups on the phenyl ring result in a steric clash between the ChiCAAC ligand and the substrate in both key transition states, leading to a $\Delta\Delta G_{(R,S-S,R)}^{\ddagger}$ of only 0.9 kcal/mol in favor of the *S*,*R* enantiomer. Similarly, replacing the aryl moiety with a tert-butyl group predicts a switch in enantioselectivity in favor of the *R*,*S* product, although here also without any significant improvement of the overall enantioselectivity (with respect to **Ru-4**). Altogether, these predictions suggest that attaining higher enantioselectivity with these DEP-*N*-substituted RuChi-CAAC complexes will not be readily achieved by a simple modification of the steric environment at the quaternary chiral carbon of the ChiCAAC ligand.

CONCLUSIONS

To conclude, a set of 14 chiral Ru-complexes containing various ^{DEP}CAAC ligands was synthesized and separated by preparative HPLC. These complexes (at 1 mol %) were found to outperform their ^{DIPP}CAAC-Ru congeners. This was attributed to their smaller steric demand. However, the presence of syn/anti Ru-rotamers was detrimental to the chiral induction as lower enantioselectivities were observed (ranging from 17 to 80% vs 92%). Mechanistic considerations, supported by DFT calculations, highlight the importance of steric factors both during and before the enantio-determining step.

Scheme 5. (A) Proposed Propagating Species A_{syn}/A_{anti} Resulting from *anti* (*S*)-Ru-4 and *syn* (*S*)-Ru-4; (B) Energy Profile for the *E* Pathway Starting from A_{syn}/A_{anti}; and (C) Proposed Structural Considerations Accounting for the Observed Enantioselectivities[a]

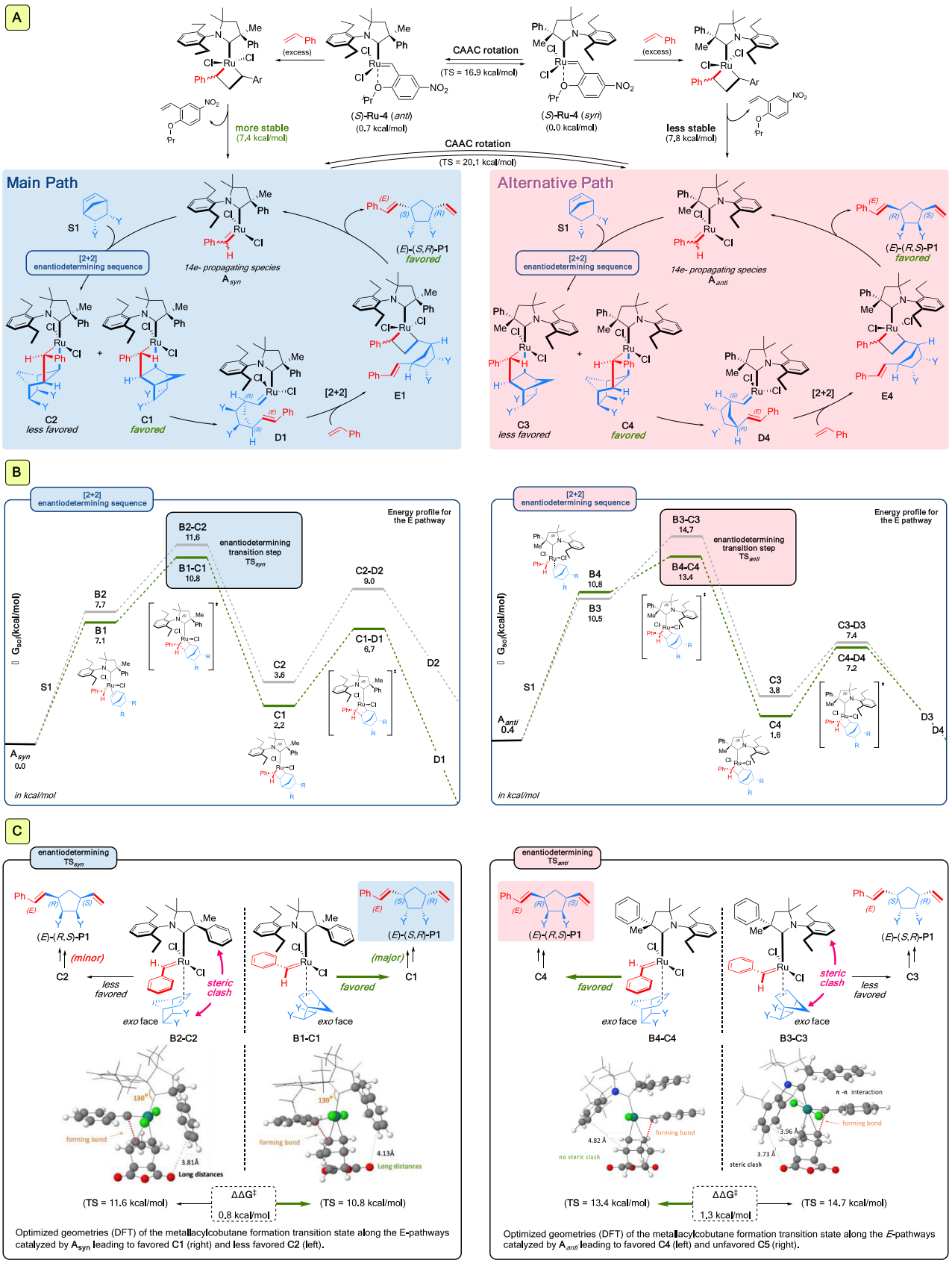

[a]Free energies (in kcal/mol) at the PBE0-D3/TZVP~SDD //PBE0-D3/SVP~SDD level are given in THF (see SI for details).

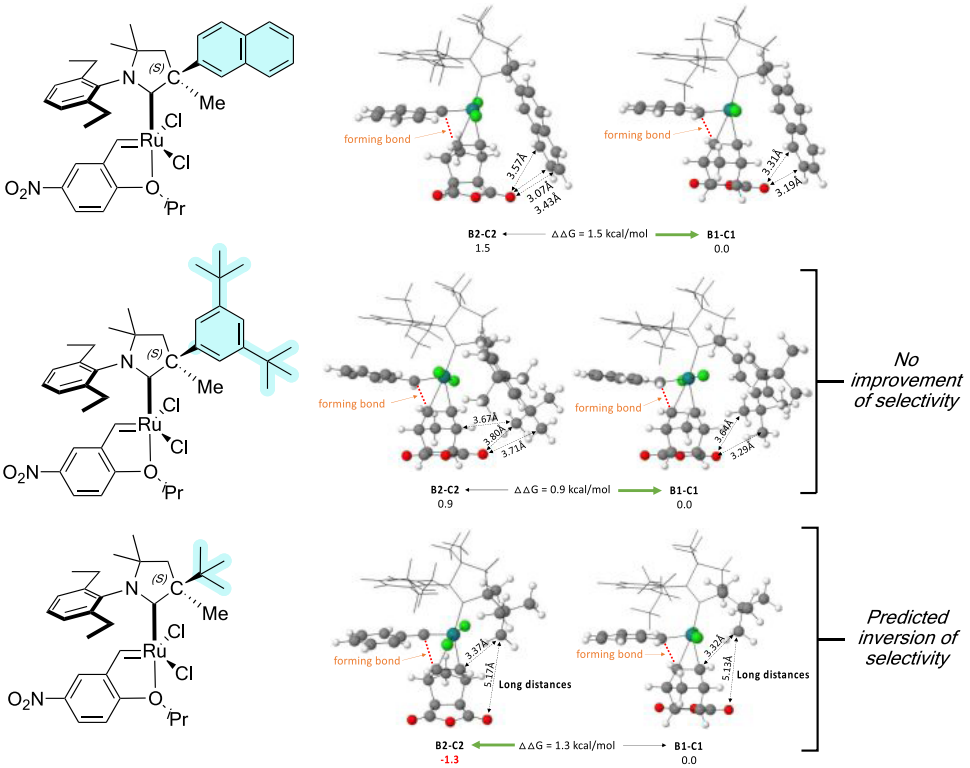

Figure 5. Predicting the effect of ligand modification over the enantio-determining transition step. Free energies (in kcal/mol) at the PBE0-D3/TZVP~SDD //PBE0-D3/SVP~SDD level are given in THF (see SI for details).

AUTHOR INFORMATION

Corresponding Authors

Guy Bertrand − *Department of Chemistry and Biochemistry, UCSD-CNRS Joint Research Chemistry Laboratory (UMI 3555), University of California, San Diego, California 92093-0358, United States*; Email: g.bertrand@ucsd.edu

Rodolphe Jazzar − *Department of Chemistry and Biochemistry, UCSD-CNRS Joint Research Chemistry Laboratory (UMI 3555), University of California, San Diego, California 92093-0358, United States;* orcid.org/0000-0002-4156-7826; Email: rjazzar@ucsd.edu

Marc Mauduit − *Ecole Nationale Supérieure de Chimie de Rennes, CNRS, ISCR UMR 6226, Univ Rennes, F-35000 Rennes, France;* orcid.org/0000-0002-7080-9708; Email: marc.mauduit@ensc-rennes.fr

Authors

Jennifer Morvan − *Ecole Nationale Supérieure de Chimie de Rennes, CNRS, ISCR UMR 6226, Univ Rennes, F-35000 Rennes, France*

François Vermersch − *Department of Chemistry and Biochemistry, UCSD-CNRS Joint Research Chemistry Laboratory (UMI 3555), University of California, San Diego, California 92093-0358, United States;* orcid.org/0000-0002-8417-8003

Ziyun Zhang − *KAUST Catalysis Center (KCC), King Abdullah University of Science and Technology (KAUST), Thuwal 23955-6900, Saudi Arabia*

Thomas Vives − *Ecole Nationale Supérieure de Chimie de Rennes, CNRS, ISCR UMR 6226, Univ Rennes, F-35000 Rennes, France;* orcid.org/0000-0001-6533-0703

Thierry Roisnel − *Ecole Nationale Supérieure de Chimie de Rennes, CNRS, ISCR UMR 6226, Univ Rennes, F-35000 Rennes, France*

Christophe Crévisy − *Ecole Nationale Supérieure de Chimie de Rennes, CNRS, ISCR UMR 6226, Univ Rennes, F-35000 Rennes, France;* orcid.org/0000-0001-5145-1600

Laura Falivene − *Dipartimento di Chimica e Biologia, Università di Salerno, 84100 Fisiciano, SA, Italy*

Luigi Cavallo − *KAUST Catalysis Center (KCC), King Abdullah University of Science and Technology (KAUST), Thuwal 23955-6900, Saudi Arabia;* orcid.org/0000-0002-1398-338X

Nicolas Vanthuyne − *Centrale Marseille, iSm2, Aix Marseille Univ., CNRS, F-13013 Marseille, France;* orcid.org/0000-0003-2598-7940

REFERENCES

(1) Grubbs, R. H. Banquet speech. NobelPrize.org. Nobel Prize Outreach AB, 2023. Mon. 13 Feb 2023. https://www.nobelprize.org/prizes/chemistry/2005/grubbs/speech/.

(2) (a) Lavallo, V.; Canac, Y.; Präsang, C.; Donnadieu, B.; Bertrand, G. Stable Cyclic (Alkyl)(Amino)Carbenes as Rigid or Flexible, Bulky, Electron-rich Ligands for Transition-Metal Catalysts: a Quaternary Carbon Atom Makes the Difference. *Angew. Chem., Int. Ed.* **2005**, *44*, 5705−5709. For a recent review on CAACs, see: (b) Soleilhavoup, M.; Bertrand, G. Cyclic (Alkyl)(Amino)Carbenes (CAACs): Stable Carbenes on the Rise. *Acc. Chem. Res.* **2015**, *48*, 256−266.

(3) Anderson, D. R.; Lavallo, V.; O'Leary, D. J.; Bertrand, G.; Grubbs, R. H. Synthesis and Reactivity of Olefin Metathesis Catalysts Bearing Cyclic (Alkyl)(Amino)Carbenes. *Angew. Chem., Int. Ed.* **2007**, *46*, 7262−7265.

(4) For a review, see: Morvan, J.; Mauduit, M.; Bertrand, G.; Jazzar, R. Cyclic (Alkyl)(amino)carbenes (CAACs) in Ruthenium Olefin Metathesis. *ACS Catal.* **2021**, *11*, 1714−1748.

(5) Selected examples: (a) Marx, V. M.; Sullivan, A. H.; Melaimi, M.; Virgil, S. C.; Keitz, B. K.; Weinberger, D. S.; Bertrand, G.; Grubbs, R. H. Cyclic Alkyl Amino Carbene (CAAC) Ruthenium Complexes as Remarkably Active Catalysts for Ethenolysis. *Angew. Chem., Int. Ed.* **2015**, *54*, 1919−1923. (b) Zhang, J.; Song, S.; Wang, X.; Jiao, J.; Shi, M. Ruthenium-Catalyzed Olefin Metathesis Accelerated by the Steric Effect of the Backbone Substituent in Cyclic (Alkyl)(Amino) Carbenes. *Chem. Commun.* **2013**, *49*, 9491−9493. (c) Gawin, R.; Kozakiewicz, A.; Guńka, P. A.; Dąbrowski, P.; Skowerski, K. Bis(Cyclic Alkyl Amino Carbene) Ruthenium Complexes: A Versatile, Highly Efficient Tool for Olefin Metathesis. *Angew. Chem., Int. Ed.* **2017**, *56*, 981−986. (d) Gawin, R.; Tracz, A.; Chwalba, M.; Kozakiewicz, A.; Trzaskowski, B.; Skowerski, K. Cyclic Alkyl Amino Ruthenium Complexes Efficient Catalysts for Macrocyclization and Acrylonitrile Cross Metathesis. *ACS Catal.* **2017**, *7*, 5443−5449. (e) Nascimento, D. L.; Gawin, A.; Gawin, R.; Gunka, P. A.; Zachara, J.; Skowerski, K.; Fogg, D. E. Integrating Activity with Accessibility in Olefin Metathesis: An Unprecedentedly Reactive Ruthenium-Indenyliden Catalyst. *J. Am. Chem. Soc.* **2019**, *141*, 10626−10631. (f) Samkian, A. E.; Xu, Y.; Virgil, S. C.; Yoon, K.-Y.; Grubbs, R. H. Synthesis and Activity of Six-Membered Cyclic Alkyl Amino Carbene−Ruthenium Olefin Metathesis Catalysts. *Organometallics* **2020**, *39*, 495−499. (g) Nagyházi, M.; Turczel, G.; Balla, Á.; Szálas, G.; Tóth, I.; Gál, G. T.; Petra, B.; Anastas, P. T.; Tuba, R.; et al. Towards Sustainable Catalysis - Highly Efficient Olefin Metathesis in Protic Media Using Phase Labelled Cyclic Alkyl Amino Carbene (CAAC) Ruthenium Catalysts. *ChemCatChem* **2020**, *12*, 1953−1957.

(6) Vermersch, F.; Oliveira, L.; Hunter, J.; Soleilhavoup, M.; Jazzar, R.; Bertrand, G. Cyclic (Alkyl)(amino)carbenes: Synthesis of Iminium Precursors and Structural Properties. *J. Org. Chem.* **2022**, *87*, 3511−3518.

(7) Pichon, D.; Soleilhavoup, M.; Morvan, J.; Junor, G.; Vives, T.; Crévisy, C.; Lavallo, W.; Campagne, J.-M.; Mauduit, M.; Jazzar, R.; Bertrand, G. The Debut of Cyclic (Alkyl)(Amino)Carbenes (CAACs) in Enantioselective Catalysis. *Chem. Sci.* **2019**, *10*, 7807−7811.

(8) (a) Morvan, J.; Vermersch, F.; Zhang, Z.; Falivene, L.; Vives, T.; Dorcet, V.; Roisnel, T.; Crévisy, C.; Cavallo, L.; Vanthuyne, N.; Bertrand, G.; Jazzar, R.; Mauduit, M. Optically Pure C1-Symmetric Cyclic(alkyl)(amino)carbene Ruthenium Complexes for Asymmetric Olefin Metathesis. *J. Am. Chem. Soc.* **2020**, *142*, 19895−19901. (b) Morvan, J.; Vermersch, F.; Lorkowski, J.; Talcik, J.; Vives, T.; Roisnel, T.; Crévisy; Vanthuyne, N.; Bertrand, G.; Jazzar, R.; Mauduit, M. Cyclic(alkyl)(amino)carbene Ruthenium Complexes for *Z*-stereoselective (Asymmetric) Olefin Metathesis. *Catal. Sci. Technol.* **2023**, *13*, 381−388.

(9) Selected book chapter on Ru-asymmetric olefin metathesis, see: Stenne, B.; Collins, S. K. *Enantioselective Olefin Metathesis in Olefin Metathesis: Theory and Pratice*; Grela, K., Ed.; Wiley-VCH: Weinheim (Germany), 2014.

(10) The use of preparative HPLC has become the most time- and cost-effective approach for enantiomer resolution at the discovery stage in the pharmaceutical industry. Chiral HPLC resolution of chiral transition-metal complexes has been reported, see: (a) Norel, L.; Rudolph, M.; Vanthuyne, N.; Williams, J. A. G.; Lescop, C.; Roussel, C.; Autschbach, J.; Crassous, J.; R Réau, R. Metallahelicenes: Easily Accessible Helicene Derivatives with Large and Tunable Chiroptical Properties. *Angew. Chem., Int. Ed.* **2010**, *49*, 99−102. (b) Hellou, N.; Jahier-Diallo, C.; Baslé, O.; Srebro-Hooper, M.; Toupet, L.; Roisnel, T.; Caytan, E.; Roussel, C.; Vanthuyne, N.; Autschbach, J.; Mauduit, M.; Crassous, J. Electronic and Chiroptical Properties of Chiral Cycloiridiated Complexes Bearing Helicenic NHC Ligands. *Chem. Commun.* **2016**, *52*, 9243−9246. (c) Hellou, N.; Srebro-Hooper, M.; Favereau, L.; Zinna, F.; Caytan, E.; Toupet, L.; Dorcet, V.; Jean, M.; Vanthuyne, N.; Williams, J. A. G.; Di Bari, L.; Autschbach, J.; Crassous, J. Enantiopure Cycloiridiated Complexes Bearing a Pentahelicenic N-Heterocyclic Carbene and Displaying Long-Lived Circularly Polarized Phosphorescence. *Angew. Chem., Int. Ed.* **2017**, *56*, 8236−8239. (d) Kong, L.; Morvan, J.; Pichon, D.; Jean, M.; Albalat, M.; Vives, T.; Colombel-Rouen, S.; Giorgi, M.; Dorcet, V.; Roisnel, T.; Crévisy, C.; Nuel, D.; Nava, P.; Humbel, S.; Vanthuyne, N.; Mauduit, M.; Clavier, H. From Prochiral N-Heterocyclic Carbenes to Optically Pure Metal Complexes: New Opportunities in Asymmetric Catalysis. *J. Am. Chem. Soc.* **2020**, *142*, 93−98. See also ref. 8

(11) Madron du Vigné, A.; Cramer, N. Chiral Cyclic Alkyl Amino Carbene (CAAC) Transition-Metal Complexes: Synthesis, Structural Analysis, and Evaluation in Asymmetric Catalysis. *Organometallics* **2022**, *41*, 2731−2741.

(12) Selected examples of structural vs. selectivity studies: (a) Sharma, A. K.; Sameera, W. M. C.; Jin, M.; Adak, L.; Okuzono, C.; Iwamoto, T.; Kato, M.; Nakamura, M.; Morokuma, K. DFT and AFIR Study on the Mechanism and the Origin of Enantioselectivity in Iron-Catalyzed Cross-Coupling Reactions. *J. Am. Chem. Soc.* **2017**, *139*, 16117−16125. (b) Romero, E. A.; Chen, G.; Gembicky, M.;

Jazzar, R.; Yu, J.-Q.; Bertrand, G. Understanding the Activity and Enantioselectivity of Acetyl-Protected Aminoethyl Quinoline ligands in Palladium-Catalyzed β-C(sp3)-H Bond Arylation reactions. *J. Am. Chem. Soc.* **2019**, *141*, 16726−16733.

(13) Selected examples of AROCM: (a) Berlin, J. M.; Goldberg, S. D.; Grubbs, R. H. Highly Active Chiral Ruthenium Catalyst for Asymmetric Cross-Metathesis and Ring-Opening Cross-Metathesis. *Angew. Chem., Int. Ed.* **2006**, *45*, 7591−7595. (b) Giudici, R. E.; Hoveyda, A. H. Directed Catalytic Asymmetric Olefin Metathesis. Selectivity Control by Enoate and Ynoate Groups in Ru-Catalyzed Asymmetric Ring-Opening/ Cross-Metathesis. *J. Am. Chem. Soc.* **2007**, *129*, 3824−3825. (c) Kannenberg, A.; Rost, D.; Eibauer, S.; Tiede, S.; Blechert, S. A Novel Ligand for the Enantioselective Ruthenium-Catalyzed Olefin Metathesis. *Angew. Chem., Int. Ed.* **2011**, *50*, 3299−3302. (d) Hartung, J.; Dornan, P. K.; Grubbs, R. H. Enantioselective Olefin Metathesis with Cyclometalated Ruthenium Complexes. *J. Am. Chem. Soc.* **2014**, *136*, 13029−13037. (e) Paradiso, V.; Bertolasi, V.; Costabile, C.; Grisi, F. Ruthenium olefin metathesis catalysts featuring unsymmetrical N-heterocyclic carbenes. *Dalton Trans.*, **2016**, *45*, 561−571.

(14) Khan, R. K. M.; O'Brien, R. V.; Torker, S.; Li, B.; Hoveyda, A. H. *Z*- and Enantioselective Ring-Opening/Cross-Metathesis with Enol Ethers Catalyzed by Stereogenic-at-Ru Carbenes: Reactivity, Selectivity, and Curtin−Hammett Kinetics. *J. Am. Chem. Soc.* **2012**, *134*, 12774−12779.

(15) Michrowska, A.; Bujok, R.; Harutyunyan, S.; Sashuk, V.; Dolgonos, G.; Grela, K. Nitro-Substituted Hoveyda−Grubbs Ruthenium Carbenes: Enhancement of Catalyst Activity through Electronic Activation. *J. Am. Chem. Soc.* **2004**, *126*, 9318−9325.

(16) Note that the synthesis of **Ru-2** was previously reported but in a lower 13% isolated yield, see ref. 5d.

(17) CHIRALPAK IE-3/IE is a polysaccharide-based column, immobilizing "amylose tris(3,5-dichloro-phenylcarbamate) to silica gel (Daicel). CHIRALPAK IF-3/IF is a polysaccharide-based column, immobilizing "amylose tris (3-chloro-4-methylphenylcarbamate)" to silica gel (Daicel).

(18) For a larger scale, the Ru-4 complex was synthesized by ourselves (see Scheme 1) following the experimental protocol previously reported in ref. 5c,d.

(19) ((a) The mixture of) *syn*/*anti* isomer was already reported in CAAC-Ru complexes, see ref. 3 and 5g. ((b) The) *syn*/*anti* ratio were unchanged after the HPLC separation. The mixture of syn/anti isomer was also reported for C_1-symmetric diaminocarbenes Ru-complexes, see: (c) Fournier, P.-A.; Savoie, J.; Stenne, B.; Bédard, M.; Grandbois, A.; Collins, S. K. Mechanistically Inspired Catalysts for Enantioselective Desymmetrizations by Olefin Metathesis. *Chem.−Eur. J.* **2008**, *14*, 8690−8695. (d) Stenne, B.; Timperio, J.; Savoie, J.; Dudding, T.; Collins, S. K. Desymmetrizations Forming Tetrasubstituted Olefins Using Enantioselective Olefin Metathesis. *Org. L ett.* **2010**, *12*, 2032−2035.

(20) Iodine complexes allowed an improvement of enantioselectivity, see for instance: Seiders, T. J.; Ward, D. W.; Grubbs, R. H. Enantioselective Ruthenium-Catalyzed Ring-Closing-Metathesis. *Org. Lett.* **2001**, *3*, 3225−3228.

(21) AROCM with exo-norbornene derivatives led to lower ees, see for instance: (a) Van Veldhuizen, J. J.; Gillingham, D. G.; Garber, S. B.; Kataoka, O.; Hoveyda, A. H. Chiral Ru-Based Complexes for Asymmetric Olefin Metathesis: Enhancement of Catalyst Activity through Steric and Electronic Modifications. *J. Am. Chem. Soc.* **2003**, *125*, 12502−12508. (b) Keitz, B. K.; Grubbs, R. H. Ruthenium Olefin Metathesis Catalysts Bearing Carbohydrate-Based N-Heterocyclic Carbenes. *Organometallics* **2010**, *29*, 403−408. See also ref. 13a